FIGURE S1

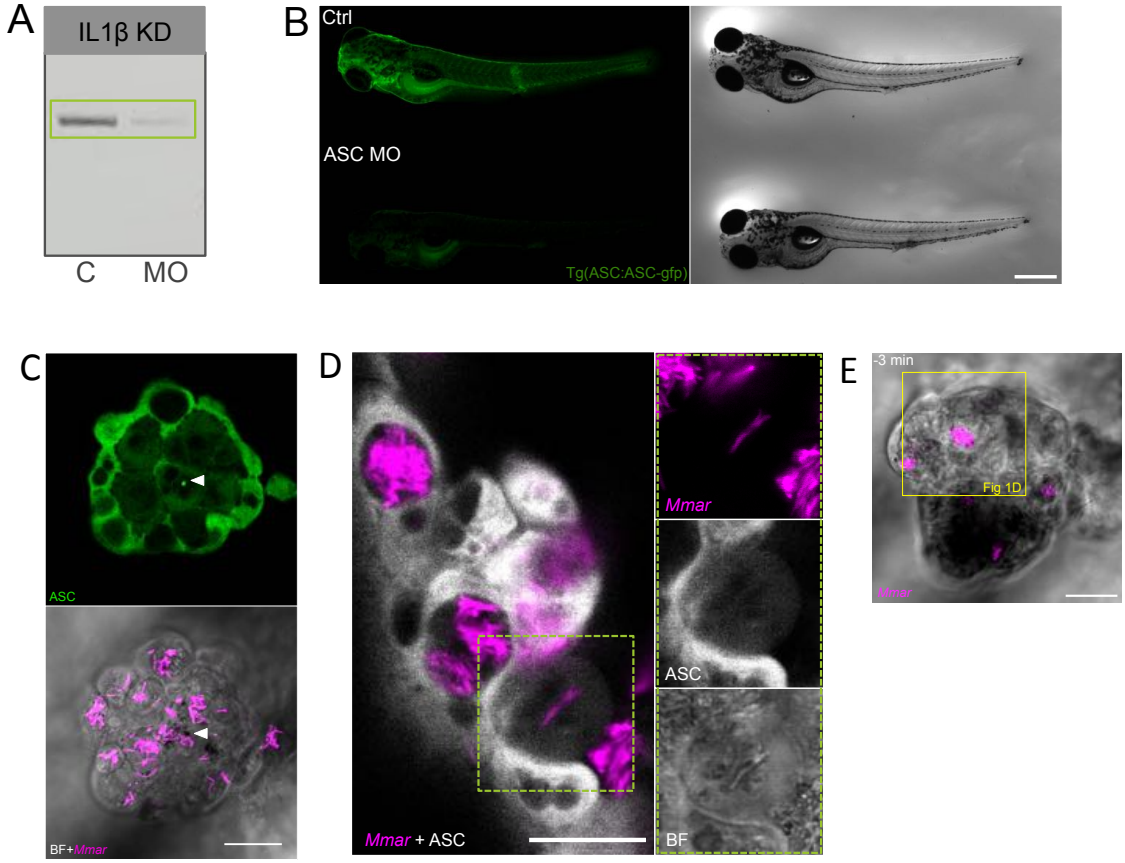

Figure S1 (related to Figure 1). Asc-independent cell death is commonly visible in zebrafish granulomas. (A) *il1β* KD efficiency was assessed by PCR on 4 dpf zebrafish DNA samples. (B) *asc* KD efficiency was assessed injecting *asc* MO into 1 cell-stage eggs from tg(*Asc*:Asc-GFP) zebrafish. Loss of Asc-GFP was assessed at 4 dpf. (C) Confocal images of a zebrafish granuloma at 3 dpi showing 1 Asc speck. (D) Confocal and BF images of Asc speck-independent cell death in zebrafish granuloma at 3dpi. (E) Confocal image of the granuloma shown in Figure 1D. Scale bars are 500 (B) and 20 (C, D, E) μm.

FIGURE S2

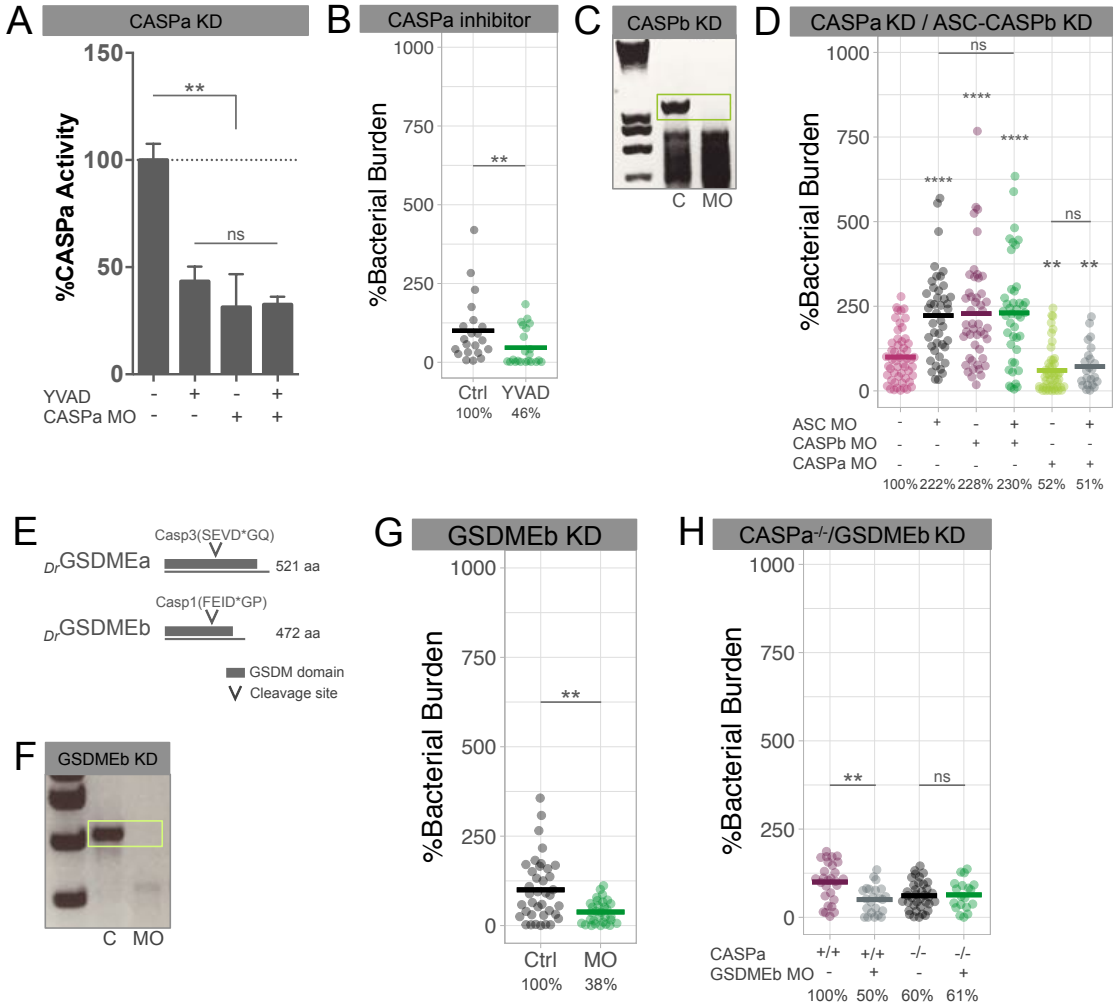

Figure S2 (related to Figure 2). Disrupting Caspa/Gsdmeb axis increases host resistance to *Mmar* infection. (A) Caspase-1 like activity in control and *caspa* KD zebrafish showing that YVAD specifically inhibits Caspa in this infection model. (B) Bacterial burden quantification after treatment with Caspa inhibitor (YVAD). (C) *caspb* KD efficiency was assessed by PCR on 4 dpf zebrafish DNA samples. (D) Bacterial burden quantification in *caspa+asc* KD and *asc+caspb* KD. (E) Schematic representing the 2 proteins with gasdermin domain in zebrafish (Gsdmea and Gsdmeb) and their caspase cleavage predicted sites. (F) *gsdmeb* KD efficiency was assessed by PCR on 4 dpf zebrafish DNA samples. (G) Bacterial burden data after transient *gsdmeb* KD in zebrafish larvae at 2 dpi (300 cfu). (H) Bacterial burden quantification in *caspa* mutants combined with *gsdmeb* KD. Mann-Whitney test (B, E) and Ordinary one-way ANOVA + Tukey´s multiple comparisons test (A, D, H), **p<0.01, ****p<0.0001.

FIGURE S3

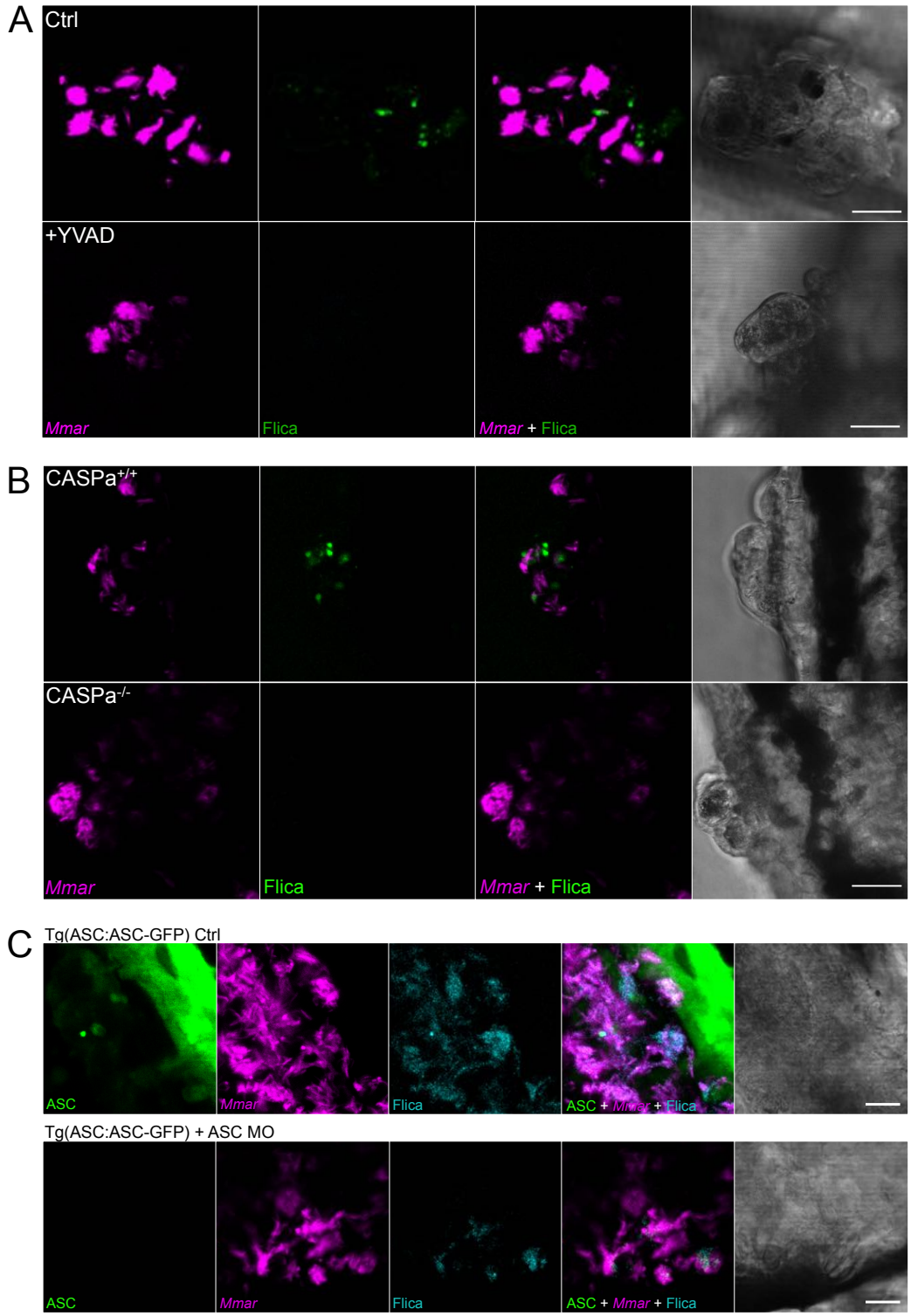

Figure S3 (related to Figure 3). *In situ* Caspa activation is Asc independent and can be specifically detected in zebrafish granulomas. (A) Confocal images showing the specificity of Flica staining after treatment with YVAD. (B) Confocal images showing the lack of Flica-positive signal in *caspa*$^{-/-}$ zebrafish larvae. (C) Confocal images showing Caspa activation (Flica) in *asc* KD *Mmar*-infected zebrafish larvae. Images are representative of >3 granulomas per condition. Scale bars are 20 (A, B, C) μm.

FIGURE S4

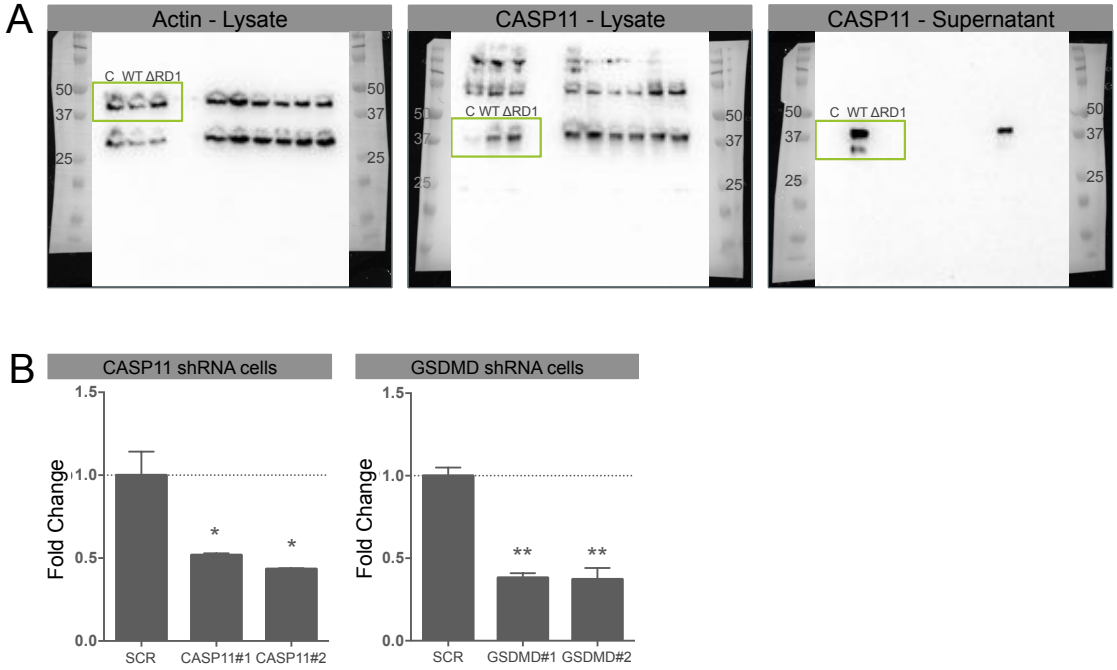

Figure S4 (related to Figure 5). Silencing of CASP11 and GSDMD in Raw264.7 macrophages supports the requirement of these proteins for *Mmar*-induced pyroptosis. (A) Full blots from Figure 5A. (B) shRNA efficiency was assessed by qPCR on Raw264.7 DNA samples. Mann-Whitney test (B), *p<0.05, **p<0.01.

FIGURE S5

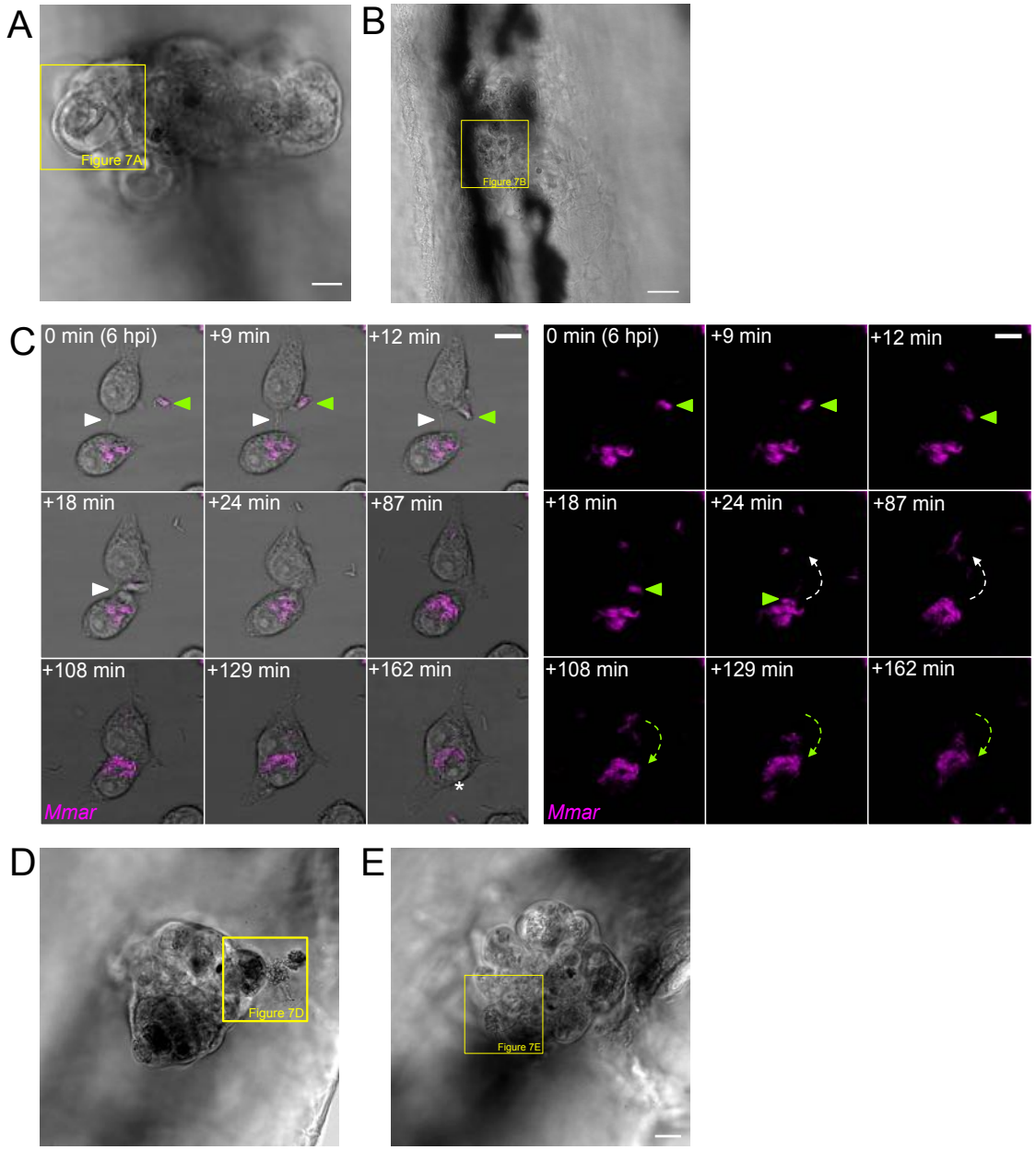

Figure S5 (related to Figure 7). *Mmar* infection induces formation of cell-in-cell structures *in vivo* and *in vitro*. (A) Zebrafish granuloma in Figure 7A. (B) Zebrafish granuloma in Figure 7B. (C) Confocal time-series showing cell-in-cell formation during *Mmar* infection (MOI=10) in Raw264.7 macrophages. Depicted cells are in contact (white arrow head). *Mmar* cluster (green arrow head) appears. Cell 1 (top cell) takes it up and transfers it inside cell 2 (bottom cell). Min 24, some bacteria from the cluster remain inside cell 1 and migrate towards the other cluster at the top of the cell (white arrow). Entosis starts min 108. Bacteria inside cell 1 migrate towards cell 2 while this cell is internalized by cell 1 (green arrow). Asterisk= cell 2 nucleus shrinkage. See also Movie 5. (D) Zebrafish granuloma in Figure 7D. (E) Zebrafish granuloma in Figure 7E. Scale bars are 10 (A, B, C, D, E) μm.

FIGURE S6

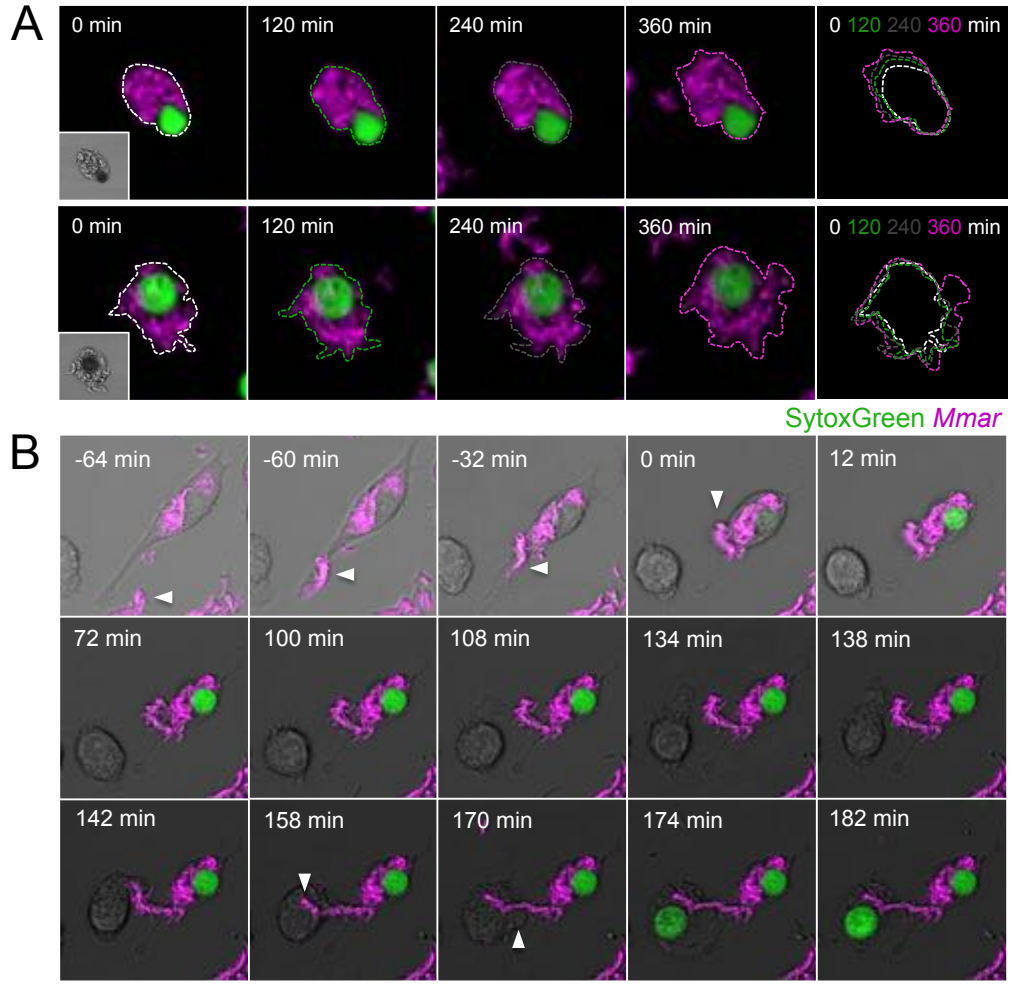

Figure S6 (related to Figure 7). Pyroptosis of infected cells leads to Mmar extracellular growth and dissemination. (A) Extracellular growth of *Mmar* after Raw264.7 cell pyroptosis during 360 min after pyroptosis. (B) Attraction of new macrophages by pyroptotic cells. New cells phagocyte *Mmar* and die via pyroptosis (Movie 6). Scale bars are 10 (A, B) μm.